ELSEVIER

Carbohydrate Research 337 (2002) 595–605

CARBOHYDRATE RESEARCH

www.elsevier.com/locate/carres

Disentangling α from β mechanical relaxations in the rubber-to-glass transition of high-sugar–chitosan mixtures

Stefan Kasapis,[a,*] Jacques Desbrières,[b] Insaaf M. Al-Marhoobi,[a] Marguerite Rinaudo[b]

[a]*Department of Food Science and Nutrition, College of Agriculture, Sultan Qaboos University, PO Box 34, Al-Khod 123, Sultanate of Oman*
[b]*CERMAV-CNRS, BP 53, 38041 Grenoble Cedex 9, Grenoble, France*

Received 7 June 2001; accepted 18 December 2001

Abstract

The occurrence of molecular motions in addition to those of the glass-transition region (α mechanism) were investigated in chitosan and a branched derivative substituted with alkyl chains having eight carbon atoms. Once hydrophobic interactions of the alkyl groups in aqueous solution were demonstrated, polymers were mixed with glucose syrup at high levels of solids. The real (G') and imaginary (G'') components of the complex dynamic modulus in high-solid mixtures were measured between 0.1 and 100 rad s^{-1} in the temperature range from -55 to 50 °C. The method of reduced variables gave superposed curves of G' and G'', which unveiled an anomaly in the dispersion of the alkylated derivative both in terms of higher modulus values and dominant elastic component of the polymeric network, as compared with the glass-transition region of chitosan. It was proposed that the new mechanical feature was due to β mechanism, and master curves of viscoelastic functions and relaxation processes were constructed to rationalize it.

Keywords: Chitosan; Alkylated derivative; Dynamic oscillation; Glass transition; β Relaxation

1. Introduction

Chitin is an important natural polymer found in the exoskeleton of crustaceans and as a component of many fungi. Commercial chitin is available at various degrees of *N*-acetylation (DA), ranging from the fully *N*-acetylated to the totally deacetylated form. Numerous food and non-food applications for chitin are foreseen and some are actively being developed.[1] At high degrees of *N*-acetylation, the polymer is only soluble in a few solvents, which limit its applications. Partial deacetylation, however, drops the DA below 50%, making the polymer soluble in aqueous acidic conditions. This product, chitosan can be considered as a copolymer containing (1→4)-linked 2-acetamido-2-deoxy-β-D-glucopyranose and 2-amino-2-deoxy-β-D-glucopyranose residues.[2]

Chitosan in aqueous solutions of dilute acids exhibits a polyelectrolyte character owing to the presence of protonated amino groups which have an intrinsic pK_0 value of 6.[3,4] Thus, the physicochemical properties of solutions of chitosan are expected to be governed by such factors as pH, ionic strength, degree of *N*-acetylation, and temperature. It is documented that the charge density along the chitosan macromolecule increases with decreasing degree of *N*-acetylation. This means that chain flexibility can be manipulated in response to DA.[5,6]

In addition, the hydrophobicity of the chitosan chain influences the steady shear viscosity and dynamic oscillatory properties of solutions.[7] The hydrophobic character can be intensified by chemical modification on the free amino groups or the hydroxyl groups present along the main chain.[8,9] Thus, chitosan derivatives having hydrophobic branches are obtained by reductive amidation following the procedure described by Yalpani and Hall.[10] This is a useful and specific method for creating a covalent bond between a substrate and the amine function of the chitosan. The aqueous solution properties of branched chitosan derivatives can be controlled by varying the degree of substitution and the pendant glycosidic functionality.[10,11]

* Corresponding author. Tel.: +968-515256; fax: +968-513418.
E-mail address: stefan@squ.edu.om (S. Kasapis).

3378-6215/02/$ - see front matter
PII: S0008-6215(02)00020-4

Alkylated chitosan chains offer an extra dimension to the investigation of relaxation and glass transition phenomena, when compared to linear macromolecules. In this laboratory, a series of linear biopolymers including agarose, κ-carrageenan, deacylated gellan, and gelatin have been subjected to dynamic mechanical measurements.[12–15] The overall objective of those studies was to elucidate the molecular mechanisms involved in the various relaxations, with special emphasis on the role played by the polymer, at levels of normal industrial use (e.g., approximately 1% for polysaccharides), in the presence of high levels of sugars (up to 86%). Following the synthetic polymer approach, horizontal superpositions of frequency sweeps obtained at constant temperature intervals yielded the master curve of viscoelasticity. This, in corroboration with mechanical cooling and heating profiles identified the 'rheological' T_g as the point between the glass-transition region and the glassy state.[16] Based on this definition, small additions of gelling biopolymer accelerate the vitrification properties of sugar with the mixture undergoing vitrification as a whole.[17]

Glass (or α) transitions were characterized by (i) following them as a function of time alone and a function of temperature alone;[18] (ii) determining the monomeric friction coefficient in relation to the molecular-weight distribution of the polymer;[19] and (iii) engineering a state of iso-free-volume that could predict the development of viscoelasticity regardless of the physicochemical characteristics of polymers.[20] Besides the α mechanism, specific mechanical dispersions known as β transitions have been documented for the rapid, rotational motions of side chains of amorphous synthetic polymers, such as poly-*n*-butyl methacrylate.[21] To our knowledge, these have not been detected in high sugar–biopolymer mixtures, and the present study is in pursuit of the elusive β transition using as a probe the alkylated chitosan molecule.

2. Experimental

Materials.—The chitosan sample was obtained from Pronova (Norway). To purify the sample, it was dissolved in 0.5 M AcOH and the pH then raised to 8.5 with 2.5 M NaOH solution. The degree of *N*-acetylation was determined by ^{1}H NMR using an AC300 Bruker spectrometer.[22] A medium of D_2O in the presence of HCl (pD ~ 4) was used to dissolve the samples to a concentration of 10 mg mL^{-1}. These were freeze-dried to exchange labile protons for deuterium atoms, as follows:[22] The chitosan solution was placed in liquid nitrogen to freeze it. The solid–gas phase change was carried out under vacuum to eliminate the presence of water molecules. Following this step, the positively charged chitosan molecule (in the NH_3^+ form) was dissolved in D_2O and freeze-dried once more. The last step was repeated three times to exchange labile protons on the macromolecular chain.

^{1}H NMR spectra were recorded at 353 K. The degree of *N*-acetylation was determined from the integral of the CH_3 signal at 1.97 ppm compared with the integral of H-1 protons which was used as the internal standard. Using this method, DA was found to be 12%. The average viscometric molecular weight was determined to be around 190,000 g mol^{-1} in 0.3 M AcOH–0.2 M NaOAc using the Mark–Houwink law.[23] C_8 alkylated derivatives were also prepared. Their structural characterization was made by NMR spectroscopy allowing the determination of the degree of substitution of the macromolecular chain and the presence of monosubstituted units.[24] The degree of substitution of alkyl groups was found to be 5%.

The glucose syrup used was a Cerestar product (Batch 01136). The dextrose equivalent of the sample, which gives the content of reducing end-groups relative to glucose as 100, is 42. Using refractometry, the total level of solids was found to be 82% and glucose syrup compositions in this work refer to dry solids. Gas permeation chromatography (GPC) analysis provided the following relationship between degree of polymerization and surface area (%) of the glucose syrup spectrum:[12]

DP1	17.54
DP2	12.99
DP3	10.55
DP4	8.79
DP5	7.29
DP6	5.28
DP7	4.78
DP8	4.21
DP9	3.19
DP10	1.96
>DP10	23.40

The GPC data indicate the purity of the material. The polydisperse nature of glucose syrup prevents crystallization and ice formation at subzero temperatures at solid contents above 70%, as demonstrated by differential scanning calorimetry and small deformation dynamic oscillation.[12,25] It is a clear solution, which transforms gradually into a clear glass upon cooling. Thus, the rheological glass-transition temperature of the material was found to be −25.3 °C at 83% solids, which achieves values of storage modulus of $10^{9.2}$ Pa at −40 °C and frequency of 1 rad s^{-1}.[48] Glucose syrup is suitable for the characterization of the structural properties of polysaccharides in a high-solid environment and hence, it has been used to unveil the mechanical spectra of deacylated gellan and high methoxy pectin.[14,49]

Methods

Alkylation reaction. Preparation of chitosan derivatives in our work involves the reaction of the amine function of the chitosan and an aldehyde function. In general, the reaction of substitution of polymers is not homogeneous. Indeed, many reactions on cellulose or starch, for example, are performed in heterogeneous conditions and the chemical modification can be observed only on the accessible sites of the macromolecular chain. Due to lack of accessibility, a blockwise substitution distribution is obtained and the compound is structurally inhomogeneous. We have developed an alkylation procedure for performing homogeneous chemical reactions. The procedure is advantageous in the sense that it uses sodium cyanohydroborate ($NaCNBH_3$), a reactive and selective reducing agent as compared to sodium hydroborate ($NaBH_4$), selephenol (PhSeH) or pentacarbonyl ions in alcoholic potassium hydroxide. $NaCNBH_3$ is stable in acidic media, with the hydrolysis rate at pH 3 being lower than with other common reducing agents and at pH 7 it is only 0.5 mol% in 24 h.[26] Moreover, the reduction of the iminium ion by the BH_3CN^- anion is rapid at pH values between 6 and 7, with the reduction of aldehydes or ketones being negligible at this pH range, but the latter accelerates at pH values less than 3.5.

In the alkylation procedure used;[24] chitosan (2 g) was dissolved in 130 mL of 0.2 M AcOH and 80 mL of ethanol was added to allow solvation of the aldehyde used for alkylation. After complete dissolution, the pH was adjusted to 5.1 to avoid precipitation of the macromolecules. The optimal pH range was between 4 and 8. The solution of the aldehyde in EtOH was added at the required ratio prior to an excess of $NaCNBH_3$ (3 mol per chitosan monomole). The mixture was stirred for 24 h at rt and the alkylated chitosan was then precipitated using EtOH after the pH had been adjusted to 8 with NaOH solution. The precipitate was subjected to repeated washings using EtOH–water mixtures with increasing EtOH content from 70 to 100% v/v.

Rheological investigation.—This was performed by using the ARES, the Advanced Rheometric Expansion System (Rheometric Scientific, Piscataway, NJ, USA), which is a controlled strain rheometer. ARES has two force rebalance transducers (FRT) covering a torque range of 0.02–2000 g cm. FRT transducers are air-lubricated and essentially non-compliant. Nevertheless, it was established that any inherent machine compliance was insufficient to significantly offset measured values from the high-modulus glass systems. This was achieved by progressive adjustment of geometry settings whilst measuring samples of intermediate and high known modulus, namely: polydimethylsiloxene (PDMS) at 30 °C ($G_c = 2.5 \times 10^4$ Pa) and ice at -5 °C ($G' = 10^9$ Pa). Thus, maximum plate diameter (5 mm) and minimum gap (4 mm) consistent with accurate results could then be determined. Particular care was taken during preparation and loading of samples. These were analyzed in triplicate as a function of temperature and frequency of oscillation, yielding reproducible results within a 3% margin. When plotting on a double logarithmic scale, as in Fig. 4, replicates were effectively indistinguishable from each other.

For precise control of the sample temperature, an air convection oven was used. The oven has a dual element heater with counter-rotating air flow covering a wide temperature range of -60 to 160 °C. Samples were loaded onto the preheated plate of the rheometer and were cooled to -55 °C at a scan rate of 1 °C min^{-1}. Then they were subjected to an oscillation of a set frequency (1 rad s^{-1}) whilst heating at the same rate to 50 °C. Sample softening with increasing temperature led to a spectacular drop in the values of shear modulus which requires adjustment of the applied strain from 0.0008 to 2% for accurate monitoring of the rubber-to-glass transition. In a second repeat of experiments, frequency sweeps of 0.1–100 rad s^{-1} were obtained at temperature intervals of 4 °C for implementation of the time–temperature superposition principle.[27] Thus readings of the rigidity/storage modulus (G'), viscous/loss modulus (G''), and complex dynamic viscosity (η^*) variation with temperature and frequency were obtained.

3. Results and discussion

Hydrophobic thermogelation of chitosan and alkylated derivative.—In the present work, a case is made for correlating mechanical dispersion phenomena to identifiable segments of the linear chitosan molecule and the alkylated counterpart in the presence of a high sugar environment. In the main, the argument was based on the observation in the synthetic polymer research that at least two distinct dispersions could be found in polymers. One dispersion reflects a process corresponding to the glass-transition region or α relaxation at which the main polymer chain is thought to acquire considerable mobility.[28] At temperatures of the glass-transition region, the viscoelastic nature of the material gives rise to a predominantly viscous behavior. There is also the second process or β transition, which is attributed to the mobility of side chains, with possible localized interactions with immediately adjacent parts of the main chain.[29]

To evaluate the accuracy of the foregoing statement in biological macromolecules, we engineered a branched chitosan molecule but, beforehand, it was necessary to familiarize ourselves with the structural properties of the system in an aqueous environment. Fig. 1(a) and (b) illustrate mechanical spectra (variation of G', G'', and η^* with frequency of oscillation (ω)) for

4% chitosan at low (15 °C) and high (70 °C) temperatures, respectively. These were prepared in a solvent medium of 0.3 M AcOH–0.05 M NaOAc. The spectrum at low temperature demonstrates a predominant liquid-like character, with both moduli increasing steeply and dynamic viscosity decreasing rapidly with increasing ω. Although $G'' > G'$, moduli converge at high frequency thus demarcating the end of the flow region leading to a pseudoequilibrium plateau at frequencies beyond the experimentally accessible range.[30]

The high temperature spectrum (Fig. 1(b)) demonstrates the passage from the flow region to a predominantly elastic response ($G' > G''$), with moduli showing reduced frequency dependence, as compared with traces in Fig. 1(a). The gel-like character is intensified once alkyl branches are grafted on the chitosan molecule. Fig. 1(c) reproduces the mechanical spectrum of chitosan modified with C_8 alkyl side chains at a degree of substitution of 5%. This is typical of a cohesive gel network, with $G' > G''$, the elastic response showing no significant frequency dependence and $\log \eta^*$ versus $\log \omega$ descending steeply with a slope close to -1. Qualitatively, the viscoelastic characteristics of a high-molecular weight polymer depend on configuration rearrangements between intermolecular associations (short) and beyond associations (long). The former can be important in the glass-transition region whereas the latter dominate in the flow region.[31] At intermediate times or frequencies, i.e., in the plateau zone, neither would make a substantial contribution to relaxation, with G' being quite independent of time and losses being small (deep minimum of G'' in Fig. 1(c)).

The molecular origin of thermogelation of chitosan and its derivative is, of course, very different from the gelation behavior of naturally occurring polysaccharides. In the latter, network formation is due to direct interactions between macromolecules supported by hydrogen bonds and electrostatic forces.[32] Polysaccharide

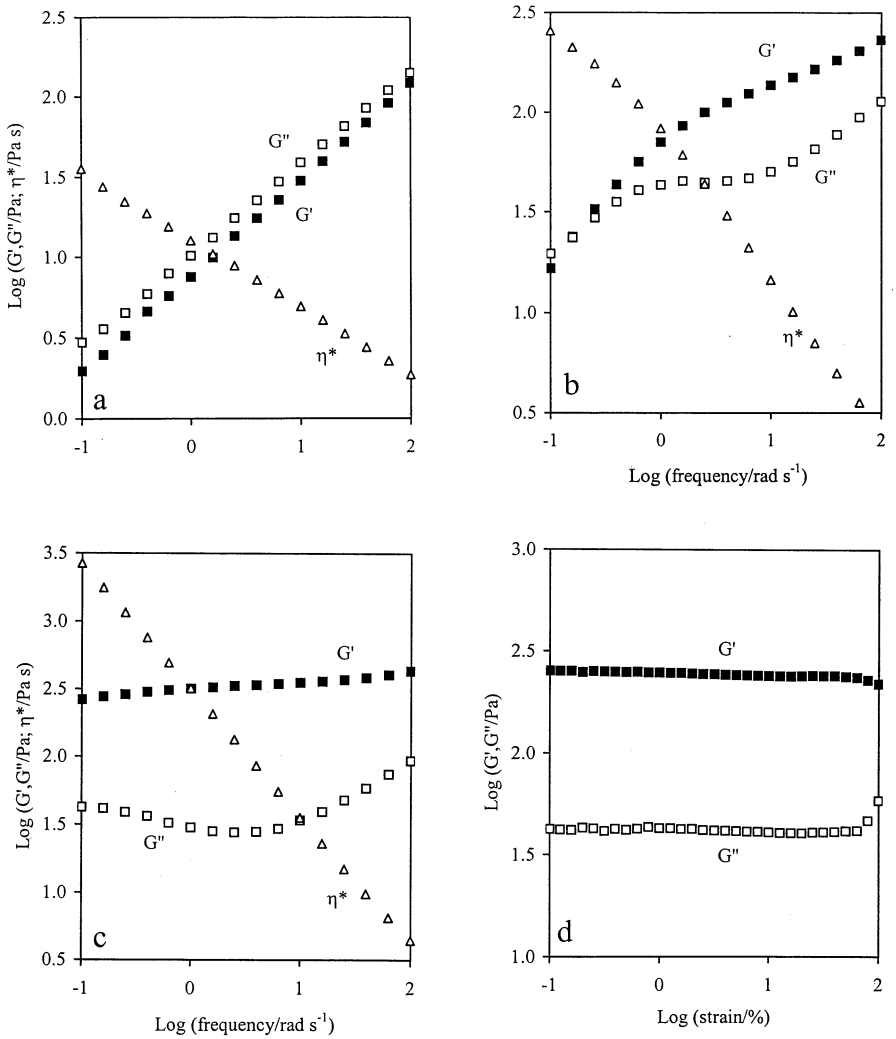

Fig. 1. Frequency dependence of G', G'' and η^* for 4% chitosan at 15 °C (a) and 70 °C (b), 4% C_8 alkylated derivative at 70 °C (c), and strain dependence of G' and G'' for the alkylated derivative at 70 °C (d). Solvent medium: 0.3 M AcOH–0.05 M NaOAc.

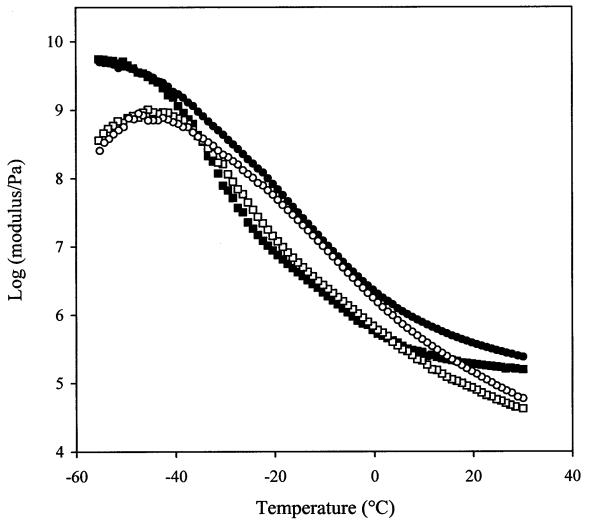

Fig. 2. Temperature dependence of shear moduli for 2% chitosan plus 73% glucose syrup (G' ■; G'' □) and 2% C_8 alkylated derivative plus 73% glucose syrup (G' ●; G'' ○) in 0.3 M AcOH–0.05 M NaOAc. Scan rate: 1 °C min^{-1}; frequency: 1 rad s^{-1}.

gelation at high temperatures has been observed previously for methyl and hydroxypropylmethyl derivatives of cellulose.[33,34] It is generally agreed that during heating, the hydrophobic substituents of the polysaccharide chain will disrupt the water cages surrounding them and cluster together in coherent structures. One piece of direct evidence from our system in favor of this interpretation, is that the increased hydrophobic character of alkylated chitosan leads to stronger gels in Fig. 1(c), as compared to those in Fig. 1(b). Finally, the failure properties of the network of the alkylated chitosan, under progressively increasing amplitude of oscillatory shear are illustrated in Fig. 1(d). It is clear that the strains used in this investigation (up to 2%) fall well within the region of linear viscoelastic response (i.e., where moduli are independent of the applied strain). Breakdown begins at about 80%, which is congruent with the breaking pattern of the 'rubbery' network of gelatin.[35]

Temperature dependence of viscoelastic behavior of high sugar–chitosan mixtures and alkylated derivative.—The mechanical spectra in Fig. 1 indicate increasing thermogelation of chitosan owing to the hydrophobic character of the alkyl substituents in an aqueous environment. Next, we modified the 'solvent quality' by replacing most of the water with glucose syrup, and then reported on the thermal/frequency dependence of viscoelasticity observed for the high solids mixtures. Fig. 2 illustrates the temperature-course of rheological changes of the two mixtures, namely, 2% chitosan and the 2% C_8 alkylated derivative in the presence of 73% glucose syrup and 0.3 M AcOH–0.05 M NaOAc (in both cases the total level of solids is 75%).

At the upper range of temperatures (> 10 °C), part of the plateau zone is unveiled, with the storage and loss modulus values of both samples converging at $10^{5.3}$ and $10^{4.7}$ Pa, respectively. The characteristic features of viscoelastic properties in this zone are due to intermolecular associations of the polymeric backbone of chitosan, which for both materials averages a viscometric molecular-weight value of 190,000 g mol^{-1} (see Materials Section). Configurational changes of segments between these associations are rapid but there is no rearrangement of associations in the plateau zone leading to constant values of shear modulus at the top experimental temperatures in Fig. 2.

At the opposite end of the accessible temperature range (< -35 °C), the glassy zone makes its appearance, with the values of G' approaching $10^{9.8}$ Pa and those of G'' going through a maximum of 10^9 Pa. Such a spectacular increase in viscoelastic functions cannot be described by configurational rearrangements, which are not possible, and the glassy zone develops a predominantly elastic rather than a viscous character. Instead, the resistance to motion depends on details of the local geometry, i.e., stretching and bending of chemical bonds mainly of the polymeric backbone. These, of course, are identical for chitosan and the alkylated derivative leading to overlapping values of shear modulus at the bottom experimental temperatures in Fig. 2.

Between the plateau and the glass-like consistency, the transition zone of linear synthetic polymers makes its appearance.[36] The dependence of viscoelastic functions on temperature is most spectacular, and this phenomenon is seen in Fig. 2 for the chitosan–glucose syrup mixture covering a modulus range of about four orders of magnitude. Viscoelastic behavior is characterized by a dominant viscous response ($G'' > G'$) owing to configurational changes of regions of the macromolecule, which are shorter than the distance between intermolecular associations. However, the chitosan derivative shows a sharper increase in shear moduli at the same temperature range, a result that should be attributed to the introduction of alkylated substituents to the polymeric backbone. Furthermore, there is a complete reversal of the viscoelastic phase, with the elastic process remaining dominant from the beginning to the end of the experimental routine. This complexity of behavior prompted us to carry out a fuller investigation in addition to the classic WLF/free volume analysis described in the following section.

Reduced dynamic data of α mechanical relaxations and the glassy state.—Examination of shear moduli as a function of temperature at constant frequency represents an obvious procedure of non-destructive rheological analysis and it has been undertaken for amorphous synthetic polymers.[37] Pictorial rheology is congruent with the thermal profile of chitosan–glucose syrup mixture in Fig. 2, thus arguing that our system undergoes

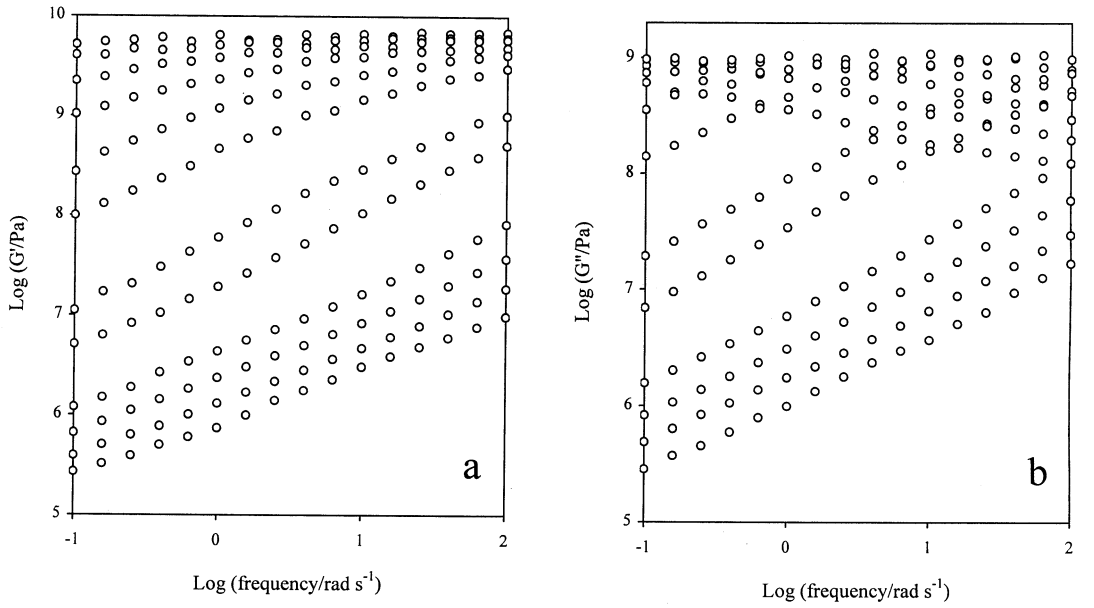

Fig. 3. Selected frequency sweeps of (a) storage modulus and (b) loss modulus for 2% chitosan plus 73% glucose. Top curve is taken at −55 °C; other curves successively downward, −51, −47, −43, −39, −35, −27, −23, −15, −11, −7 and −3 °C, respectively.

a mechanical rubber-to-glass transition. In these cases, headway is made by the separation of the variables of frequency and temperature assuming that all relaxation times depend identically on temperature.[38] According to this assumption, the effect of a change in temperature on shear modulus is primarily to shift the frequency scale.

In our work, the time–temperature equivalence was implemented using the method of reduced variables,[39] as follows: values of G' and G'' were obtained in double logarithmic plots against frequency covering a spectrum of 0.1–100 rad s^{-1}. Selected numerical data are recorded in Fig. 3. They range from −55 to −3 °C and were obtained at constant temperature intervals of 4 °C. Then, a temperature (−15 °C) was chosen arbitrarily within the glass-transition region to serve as the reference point and the remaining mechanical spectra were shifted horizontally along the logarithmic frequency axis until they fell into a smooth master curve. Reduced double logarithmic plots of storage (G'_p) and loss (G''_p) modulus against the frequency of oscillation are given in Fig. 4, clearly demarcating the glass-transition region and the glassy state. Data at all temperatures and frequencies superpose well, indicating that the assumption of equal temperature dependence of mechanical relaxations holds for the chitosan–glucose syrup system. Fig. 4 also reproduces the dynamic mechanical properties of polyisobutylene, covering ranges of frequency and temperature within which the properties change to those characteristic of a hard glass.[46] The similarity between the master curves of the biological and synthetic materials is rather spectacular, thus further supporting the concept of glass transition in the chitosan–co-solute mixture.

The master curve in Fig. 4 allowed estimation of a_T, the reduction factor, expressing the change of all relaxation times with temperature. Values of a_T were in excellent agreement for both traces of storage and loss modulus. In Fig. 5(a), the factor a_T is plotted logarithmically against the temperature range covering the glass-transition region (α mechanical relaxations).

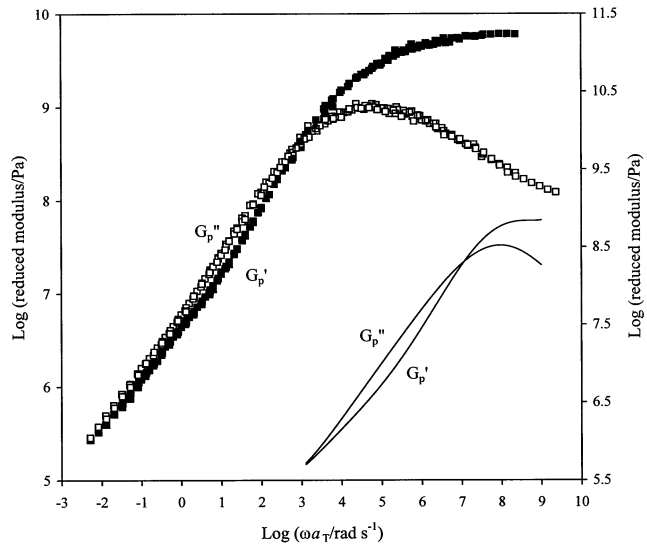

Fig. 4. Master curve of G'_p and G''_p (symbols) as a function of reduced frequency for 2% chitosan plus 73% glucose syrup generated from the data in Fig. 3 using −15 °C as the reference temperature (left y axis). Similar data for polyisobutylene (lines) are shown on the right y axis.[46]

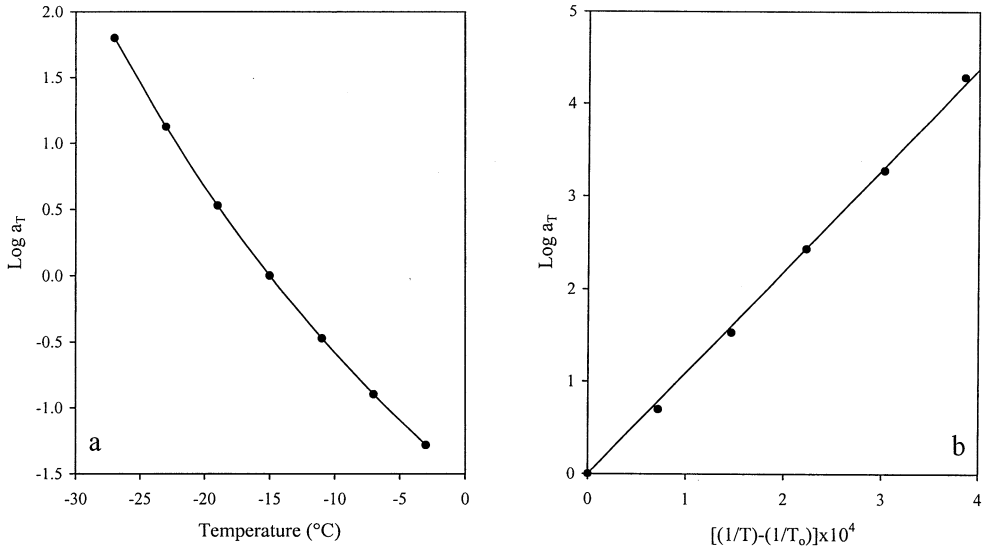

Fig. 5. Temperature dependence of shift factors in the glass-transition region (a) and the glassy state (b) for 2% chitosan plus 73% glucose syrup. The curve and straight line represent the predictions of the WLF and Andrade equations, respectively.

Log a_T is zero at -15 °C because, as mentioned in the preceding paragraph, this was arbitrarily chosen to be the reference temperature. The reduction factor is not an exponential function of the reciprocal absolute temperature but the empirical values can be fitted to the Williams–Landel–Ferry (WLF) equation which has been proved to be widely applicable in synthetic polymer research:[40]

$$\log a_T = -\frac{C_1^0(T-T_0)}{C_2^0+T-T_0} \quad (1)$$

In terms of the theory of free volume,[41] the parameters C_1^0 and C_2^0 correspond to $B/2.303f_0$ and f_0/a_f, respectively, and B for simplicity is taken to be equal to one; f_0 is the fractional free volume, namely, the ratio of free volume to total volume per gram of material at an arbitrary reference temperature T_0, and α_f is the thermal expansion coefficient of the material. As shown in Fig. 5(a), there is very good agreement between the values of factor a_T and the predictions of the WLF/free volume theory, which allows estimation of the rheological T_g (-36.5 °C) for the chitosan–glucose syrup mixture. Furthermore, the fractional free volume at T_g (f_g) and the thermal expansion coefficient were found to be 0.034 and 6.8×10^{-4} deg^{-1}, respectively, i.e., according to experience with synthetic polymers.[38]

The value of the rheological T_g for the chitosan–sugar mixture is higher than that reported for single sugar preparations. The latter was recorded to be -45.4 °C for a concentrated sugar solution of 80% solids,[14] a result which suggests that small additions of polysaccharide (2% chitosan in our case) accelerate vitrification by creating a three-dimensional structure, thus leading to molecular immobilization. The phenomenon appears to be universal, since small additions of κ-carrageenan and deacylated gellan to high levels of sugar also alter dramatically the glass-transition temperature of single sugar preparations.[50] The acceleration of vitrification properties is assisted by the presence of stoichiometric amounts of added potassium and calcium ions for the κ-carrageenan and deacylated gellan gels, respectively, which stabilize the polysaccharide network through additional electrostatic interactions. All in all, the increase in the values of T_g of co-solute in the presence of gelling polysaccharides should be due to the formation of a three dimensional network that leads to molecular immobilization and reduced rates of diffusion in the gel.

The WLF equation becomes inapplicable at temperatures lower than the glass-transition region. As shown in Fig. 5(b), the factor a_T is an exponential function of $1/T$, so the customary logarithmic form with a constant energy of activation (E_a) can be used for calculating numeral values. Thus using the Andrade equation:[42]

$$\log a_T = \frac{E_a}{2.303R}\left(\frac{1}{T}-\frac{1}{T_o}\right) \quad (2)$$

E_a, which is independent of temperature, was estimated to be 209.3 kJ mol^{-1} for an elementary flow process in the glassy state. In Fig. 5(b), the value of log a_T is zero at -35 °C chosen as the reduction temperature for graphical purposes.

The theory of free volume predicts that the glass-transition temperature is reached when the fractional free volume is about 3% of the total volume of an amorphous material.[38] This should occur at the low-temperature end of the glass-transition region since at temperatures far above the vitrification point or in the rubbery region, the proportion of free volume is far higher, perhaps 30% of the total volume, and viscoelas-

tic properties can be correlated with chemical structure. Gratifyingly, the value of rheological T_g (-36.5 °C) calculated via the WLF equation coincides with the passage from the glass-transition region to the glassy state in the thermal profile of the chitosan–glucose syrup mixture (G' becomes equal to G'' at -36 °C in Fig. 2). Mechanistically, this ascribes physical significance to the rheological T_g as an index of the transformation from free-volume derived effects in the glass-transition region to the process of an energetic barrier to rotation in the solid-like environment of the glassy state.

The working hypothesis and representation of results for β mechanical relaxations.—The glass-transition region of the chitosan–glucose syrup mixture exhibits dominant viscous mechanics in Fig. 2 and in the basic function of time (or frequency) shown in Fig. 4. Using the combined framework of the WLF/free volume theory, viscoelastic features were attributed to vibrational motions flexing over several segments of the polymeric chain. It appears, however, that the effect of introducing alkyl substituents to the chitosan chain is to produce changes of kind rather than just magnitude in the characteristic mechanical properties of the system. A cursory inspection of Fig. 2 unveils the atypical structural features of the C_8 alkylated derivative in terms of reinforced mechanical response and dominant elastic component of the polymeric network in the middle range of temperatures.

To quantify the contribution of alkyl substituents to the overall mechanical dispersion, frequency sweeps of storage and loss modulus were obtained for the alkylated derivative–glucose syrup mixture (Fig. 6), covering the temperature range of the glass-transition region observed in the chitosan–glucose syrup mixture. Then, the values of G' and G'' of the chitosan (glass-transition region in Fig. 3) were subtracted from G' and G'' of the alkylated derivative (Fig. 6) at corresponding frequencies (from 0.1 to 100 rad s^{-1}) for each experimental temperature. Logarithmic plots of the ensuing values of G' and G'' at different temperatures could be superposed by horizontal shifts at the reference temperature of -15 °C. As far as we are aware, Fig. 7 illustrates the first master curve of β mechanical relaxations in biological macromolecules. The data are in good agreement with the master curve for the β mechanism of polyethyl methacrylate, reproduced in Fig. 7 from compliance data found in Ref. 47, taking into account that the complex modulus and the complex compliance are reciprocally related.

The method of reduced variables proved to be applicable within the range of temperatures and frequencies of the transformation from the rubbery to the glassy consistency where, it appears, that the modulus contributions of the secondary mechanism are comparatively substantial. This allowed derivation of the usual arbitrary shift factors, with the same values of a_T superposing both the elastic and viscous functions of the master curve at each temperature. As shown in Fig. 8, log a_T of the β mechanical dispersion is a linear function of the reciprocal absolute temperature with a gradient corresponding to an apparent energy of activation of 309.8 kJ mol^{-1}. Clearly, the temperature dependence of the relaxation times associated with the secondary mecha-

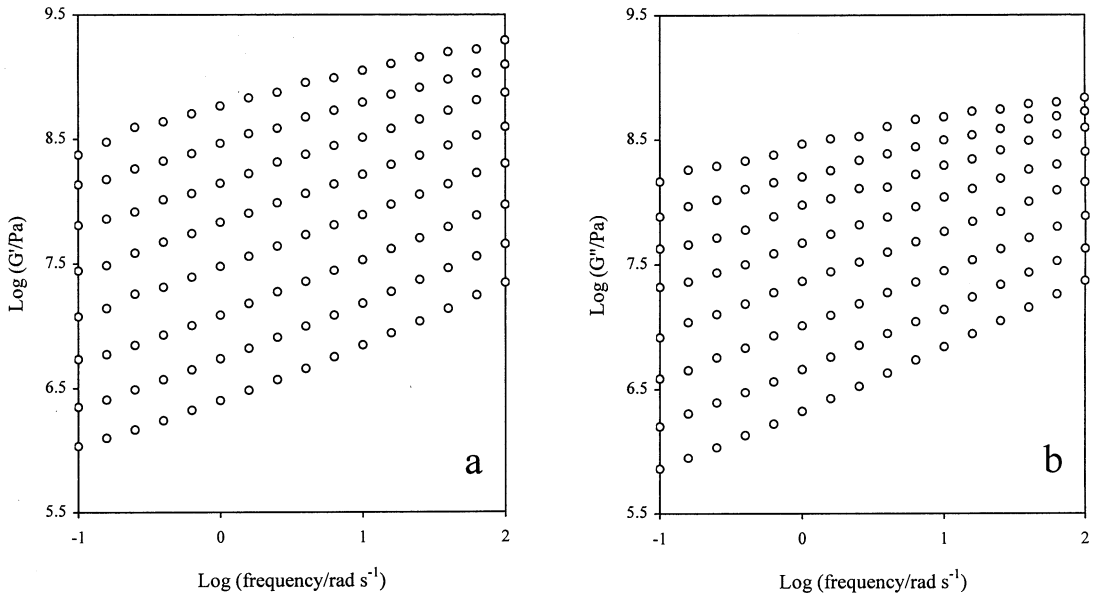

Fig. 6. Frequency sweeps of (a) storage modulus and (b) loss modulus for 2% C_8 alkylated chitosan plus 73% glucose syrup covering the α and β mechanisms. Top curve is taken at -31 °C; other curves successively downward, -27, -23, -19, -15, -11, -7 and -3 °C, respectively.

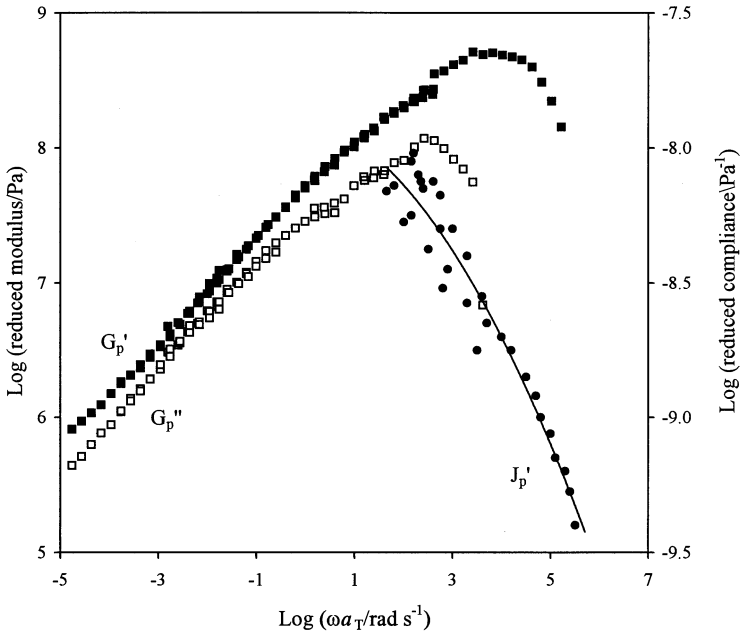

Fig. 7. Master curve of G'_p (■) and G''_p (□) as a function of reduced frequency for the β mechanism of the 2% C_8 alkylated derivative plus 73% glucose syrup using −15 °C as the reference temperature (left y axis). Similar data for the real part of the complex compliance (J'_p; ●) of polyethyl methacrylate are shown on the right y axis.[47]

nism of the alkyl side-chain motions is different from that for the primary mechanism of the chain motions of chitosan. The latter is followed by the WLF equation illustrated in Fig. 5(a), thus yielding an energy of activation which increases rapidly with decreasing temperature (data are not reproduced here), in accordance with previous observations on synthetic and biological macromolecules.[18,38]

Finally, an attempt was made to obtain a hierarchical correlation between the different characteristics of the α and β mechanical relaxations of our system in the time continuum. In doing so, the second approximation formulas of Williams and Ferry were used to derive the distribution function of relaxation times (Φ) from dynamic mechanical measurements on our system. In the past, this approach has been proved to be particularly useful because other functions, such as stress relaxation and the steady-flow viscosity, can be readily calculated from it.[43] Details on the derivation of Φ have been given previously, which in its refined form, stands as follows:[44,45]

$$\Phi_{\tau=1/\omega} = AG'\left(1-\left|\frac{d\log G'}{d\log\omega}-1\right|\right) \quad (3a)$$

$$\Phi_{\tau=1/\omega} = BG''\left(1-\left|\frac{d\log G''}{d\log\omega}\right|\right) \quad (3b)$$

The factors A and B involve gamma functions of m, which is the second derivative of the experimental quantities of storage and loss modulus with respect to time or frequency:

$$A = (1+|m-1|)/2\Gamma\left(2-\frac{m}{2}\right)\Gamma\left(1+\frac{m}{2}\right) \quad -2\le m\le 2 \quad (4a)$$

$$B = (1+|m|)/2\Gamma\left(\frac{3}{2}-\left|\frac{m}{2}\right|\right)\Gamma\left(\frac{3}{2}+\left|\frac{m}{2}\right|\right) \quad -1\le m\le 3 \quad (4b)$$

Fig. 9 illustrates the outcome of such calculations for the two mechanisms in the chitosan–glucose syrup and alkylated derivative–glucose syrup mixtures. The agreement between calculations from the storage and loss modulus for each molecular mechanism is extremely

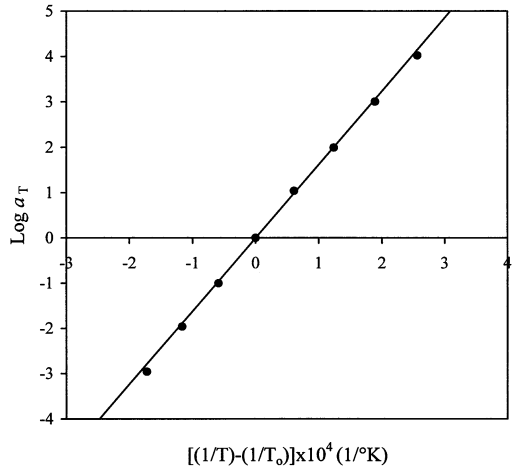

Fig. 8. Temperature dependence of shift factors for the β mechanism of the 2% C_8 alkylated derivative plus 73% glucose syrup. The straight line represents the predictions of the Andrade equation.

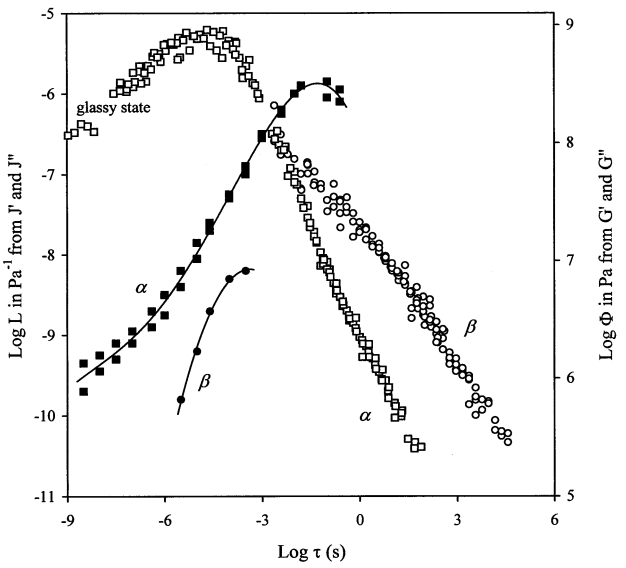

Fig. 9. Derivation of the distribution function of relaxation times (Φ) from storage and loss modulus for the α mechanism of chitosan and the backbone chain of the alkylated derivative, β mechanism of the alkyl side chains of the chitosan derivative, and the glassy state for both chitosan and the derivative (right y axis). Similar retardation spectra (L), derived from J' and J'', of the two mechanisms for poly-*n*-butyl methacrylate are shown on the left y axis (filled symbols).[21]

encouraging. Thus, the distribution function normalized modulus readings for the entirety of the relaxation spectrum, although at a single time (or frequency) of measurement, G' and G'' are independent from each other. The overall relaxation spectrum combines the two individual mechanisms reduced to -15 °C. The β mechanism lies relatively to the right of the α mechanism, but it becomes increasingly submerged by the α curve at short relaxation times. At extremely short time-scales, the glassy state makes its appearance and achieves a maximum in the distribution function. It then diminishes rapidly since the contribution to 'instantaneous rigidity' between $\ln \tau$ and $\ln \tau + d \ln \tau$ is negligible in the glassy state. Similar disentanglement of the two mechanisms has been reported for the vitrification properties of poly-*n*-butyl methacrylate (Ref. 21 and Fig. 9). Retardation spectra were calculated from the real and imaginary parts of the complex compliance but the relative positions of the α and β transitions in the time continuum are consistent with our data shown in Fig. 9.

4. Conclusions

It has been shown that carefully executed rheological analysis can disentangle α from β molecular relaxations of chitosan and the alkylated derivative in the presence of high levels of co-solute. For the α mechanism, the temperature dependence of the reduction factors followed an equation of the WLF form and it was attributed to the coordinated motions of the chitosan chain. For the β mechanism, the temperature dependence of the reduction factors yielded a constant energy of activation and it was attributed to the side chain motions of the alkyl substituents. The time-temperature superposition principle was utilized to demonstrate a time continuum in the viscoelastic functions of the β mechanism thus yielding a master curve. Second approximation calculations of the mechanical distribution function were employed to identify the relative locations of the two mechanisms on the time scale before they were superseded by a unifying glassy state.

Acknowledgements

The work was supported in part by the High Sugar Polysaccharide MAFF LINK project led by Professor J.R. Mitchell, University of Nottingham. We are much indebted to staff working on the LINK project and to Dr Ann Mothershaw, Sultan Qaboos University, for stimulating discussions and critical evaluation of this manuscript.

References

1. Whistler, R. L. In *Industrial Gums*; Whistler, R. L.; BeMiller, J. N., Eds.; Academic Press: San Diego, CA, 1993; pp. 601–618.
2. Goycoolea, F. M.; Argüelles-Monal, W.; Peniche, C.; Higuera-Ciapara, I. In *Novel Macromolecules in Food Systems*; Doxastakis, G.; Kiosseoglou, V., Eds.; Elsevier: Amsterdam, 2000; pp. 265–308.
3. Rinaudo, M.; Pavlov, G.; Desbrières, J. *Int. J. Polym. Anal. Charact.* **1999**, *5*, 267–276.
4. Rinaudo, M.; Pavlov, G.; Desbrières, J. *Polymer* **1999**, *40*, 7029–7032.
5. Wang, W.; Qin, W.; Bo, S. *Makromol. Chem. Rapid Commun.* **1991**, *12*, 559–561.
6. Wang, W.; Bo, S.; Li, S.; Qin, W. *Int. J. Biol. Macromol.* **1991**, *13*, 281–285.
7. Argüelles-Monal, W.; Goycoolea, F. M.; Peniche, C.; Higuera-Ciapara, I. *Polym. Gels Networks* **1998**, *6*, 429–440.
8. Moore, G. K.; Roberts, G. A. F. *Int. J. Biol. Macromol.* **1981**, *3*, 337–340.
9. Yalpani, M. *Tetrahedron* **1985**, *41*, 2957–3020.
10. Yalpani, M.; Hall, L. D. *Macromolecules* **1984**, *17*, 272–281.
11. Hall, L. D.; Holme, K. R. *J. Chem. Soc., Chem. Commun.* **1986**, *3*, 217–218.
12. Tsoga, A.; Kasapis, S.; Richardson, R. K. *Biopolymers* **1999**, *49*, 267–275.
13. Evageliou, V.; Kasapis, S.; Hember, M. W. N. *Polymer* **1998**, *39*, 3909–3917.
14. Sworn, G.; Kasapis, S. *Carbohydr. Res.* **1998**, *309*, 353–361.

15. Kasapis, S.; Al-Marhoobi, I. M. A.; Giannouli, P. *J. Agric. Food Chem.* **1999**, *47*, 4944–4949.
16. Kasapis, S. In *Functional Properties of Food Macromolecules*; Mitchell, J. R.; Hill, S. E.; Ledward, D. A., Eds.; Nottingham University Press: Nottingham, 1998; pp. 227–251.
17. Kasapis, S.; Al-Marhoobi, I. M. A. In *Gums and Stabilisers for the Food Industry* 10; Williams, P. A.; Phillips, G. O., Eds.; The Royal Society of Chemistry: Cambridge, 2000; pp. 303–313.
18. Kasapis, S.; Sworn, G. *Biopolymers* **2000**, *53*, 40–45.
19. Kasapis, S. *Food Hydrocolloids* **2001**, *15*, 631–641.
20. Kasapis, S.; Al-Alawi, A.; Guizani, N.; Khan, A. J.; Mitchell, J. R. *Carbohydr. Res.* **2000**, *329*, 399–407.
21. Child, W. C., Jr.; Ferry, J. D. *J. Colloid Sci.* **1957**, *12*, 327–341.
22. Rinaudo, M.; Le Dung, P.; Gey, C.; Milas, M. *Int. J. Biol. Macromol.* **1992**, *14*, 122–128.
23. Rinaudo, M.; Milas, M.; Le Dung, P. *Int. J. Biol. Macromol.* **1993**, *15*, 281–285.
24. Desbrières, J.; Martinez, C.; Rinaudo, M. *Int. J. Biol. Macromol.* **1996**, *19*, 21–28.
25. Ong, M. H.; Whitehouse, A. S.; Abeysekera, R.; Al-Ruqaie, I. M.; Kasapis, S. *Food Hydrocolloids* **1998**, *12*, 273–281.
26. Lane, C. F. *Synthesis* **1975**, 135–146.
27. Ward, I. M.; Hadley, D. W. *An Introduction to the Mechanical Properties of Solid Polymers*; Wiley: Chichester, 1993; pp. 84–108.
28. Etienne, S.; Lamorlette, C.; David, L. *J. Non-Cryst. Solids* **1998**, *235-237*, 628–634.
29. Perez, J.; Muzeau, E.; Cavaillé, J. Y. *Plast., Rubber and Compos. Process. Appl.* **1992**, *18*, 139–148.
30. Morris, E. R. In *Gums and Stabilisers for the Food Industry* 2; Phillips, G. O.; Wedlock, D. J.; Williams, P. A., Eds.; Pergamon Press: Oxford, 1984; pp. 57–78.
31. Ferry, J. D. *Viscoelastic Properties of Polymers*; Wiley: New York, 1980; pp. 224–263.
32. Dea, I. C. M. In *Industrial Gums*; Whistler, R. L.; BeMiller, J. N., Eds.; Academic Press: San Diego, CA, 1993; pp. 21–52.
33. Haque, A.; Morris, E. R. *Carbohydr. Polym.* **1993**, *22*, 161–173.
34. Haque, A.; Richardson, R. K.; Morris, E. R.; Gidley, M. J.; Caswell, D. C. *Carbohydr. Polym.* **1993**, *22*, 175–186.
35. Papageorgiou, M.; Kasapis, S.; Richardson, R. K. *Food Hydrocolloids* **1994**, *8*, 97–112.
36. Williams, M. L.; Ferry, J. D. *J. Colloid Sci.* **1954**, *9*, 479–492.
37. Ferry, J. D.; Fitzgerald, E. R. *Proceedings of the Second International Congress on Rheology*; Butterworths: London, 1954; pp. 140–149.
38. Ferry, J. D. *Viscoelastic Properties of Polymers*; Wiley: New York, 1980; pp. 264–320.
39. Plazek, D. J. *J. Rheol.* **1996**, *40*, 987–1014.
40. Williams, M. L.; Landel, R. F.; Ferry, J. D. *J. Am. Chem. Soc.* **1955**, *77*, 3701–3707.
41. Plazek, D. J. *J. Non-Cryst. Solids* **1991**, *131–133*, 836–851.
42. Arridge, R. G. C. *Mechanics of Polymers*; Oxford University Press: Oxford, 1975; pp. 24–50.
43. Ferry, J. D.; Williams, M. L. *J. Colloid Sci.* **1952**, *7*, 347–353.
44. Williams, M. L.; Ferry, J. D. *J. Polym. Sci.* **1953**, *11*, 169–175.
45. Kasapis, S.; Sablani, S. S. *Int. J. Biol. Macromol.* **2000**, *27*, 301–305.
46. Ferry, J. D.; Grandine, L. D., Jr.; Fitzgerald, E. R. *J. Appl. Phys.* **1953**, *24*, 911–916.
47. Ferry, J. D.; Child, W. C., Jr.; Zand, R.; Stern, D. M.; Williams, M. L.; Landel, R. F. *J. Colloid Sci.* **1957**, *12*, 53–67.
48. Kasapis, S.; Al-Marhoobi, I. M. A.; Khan, A. J. *Int. J. Biol. Macromol.* **2000**, *27*, 13–20.
49. Kasapis, S.; Al-Alawi, A.; Guizani, N.; Khan, A. J.; Mitchell, J. R. *Carbohydr. Res.* **2000**, *329*, 399–407.
50. Kasapis, S.; Mitchell, J. R. *Int. J. Biol. Macromol.* **2001**, *29*, 315–321.